

Full Length Research Paper

Analytical and experimental studies on infilled RC frames

Mehmet Baran^{1*} and Tugce Sevil²

¹Department of Civil Engineering, Kirikkale University, 71450, Yahsihan, Kirikkale, Turkey.

²Department of Civil Engineering, Maltepe University, 34857, Maltepe, Istanbul, Turkey.

Accepted 27 September, 2010

Although hollow brick infills, widely used as partition walls, are considered as non-structural members, experimental studies revealed that hollow brick infills have favourable effects on strength and stiffness of structures. In this work, analytical studies were conducted to investigate the hollow brick infill behaviour, in which infills were modeled by diagonal compression struts. Results were compared with experimental ones obtained from tests of one-bay, one or two story reinforced concrete (RC) frames, tested under both vertical and reversed-cyclic lateral loads simulating earthquake. Test frames have intentionally been constructed poorly to reflect the most common deficiencies encountered in Turkey such as strong beam-weak column connections, insufficient confinement, low-grade concrete, poor workmanship and insufficient lap-splice length. Experimental studies shows that hollow brick infills increased both strength and stiffness of RC frames. Analytical studies conducted, shows that hollow brick infills could adequately be modeled by diagonal compression struts.

Key words: Reinforced concrete, strength, stiffness, hollow brick infill, diagonal compression strut and reversed-cyclic lateral load.

INTRODUCTION

Filling reinforced concrete (RC) frames with clay tile serving as partitions are very common, especially in Turkey. In structural design process, such infills are considered as “nonstructural” members. Structure is assumed to carry horizontal loads only by the frame elements. However, it is apparent from geometrical considerations that infills also resist loads and impede deformations compatible with infilled frame action. Analytical and experimental studies shows that infilled frames have greater strength and stiffness compared to bare frames. Due to changes in stiffness and mass, dynamic characteristics of the building also change. Understanding the behaviour of infilled frames and being capable of making a satisfactory modeling of infills during structural design process will help engineers to have more realistic and economical solutions. Behaviour of infilled frames under seismic loading is complicated.

This is the most probable reason for hollow brick infills not being considered as “structural” members during the structural design process, resulting with inaccurate solutions. With this approach, natural period of building, earthquake load transferred to each beam and column, short column mechanisms that can occur and the failure mode of building under an earthquake loading can not be evaluated precisely. Since the behaviour is nonlinear and closely related to the interaction conditions between frame and infill, analytical studies should be revised and supported by experimental data. Earthquake regulations of many countries (Israel, Costa Rica, France, Algeria, European Union, Colombia, Phillipines, etc.) recommend to take the effect of infill walls into account during the design process (Kaplan, 2008).

In the experimental part of the present study, one and two-story RC frames were tested. In two-story frames, lateral load was applied at a greater height resulting in more turning effect whereas compressive and shear stresses are more dominant in one-story frames. By this way, hollow brick infill behaviour can be analyzed under tensile stresses as well as compressive and shear stresses.

*Corresponding author. E-mail: memetbaran@gmail.com. Tel: ++ (90) (318) 357 42 42 – 1254. Fax: ++ (90) (318) 357 24 59

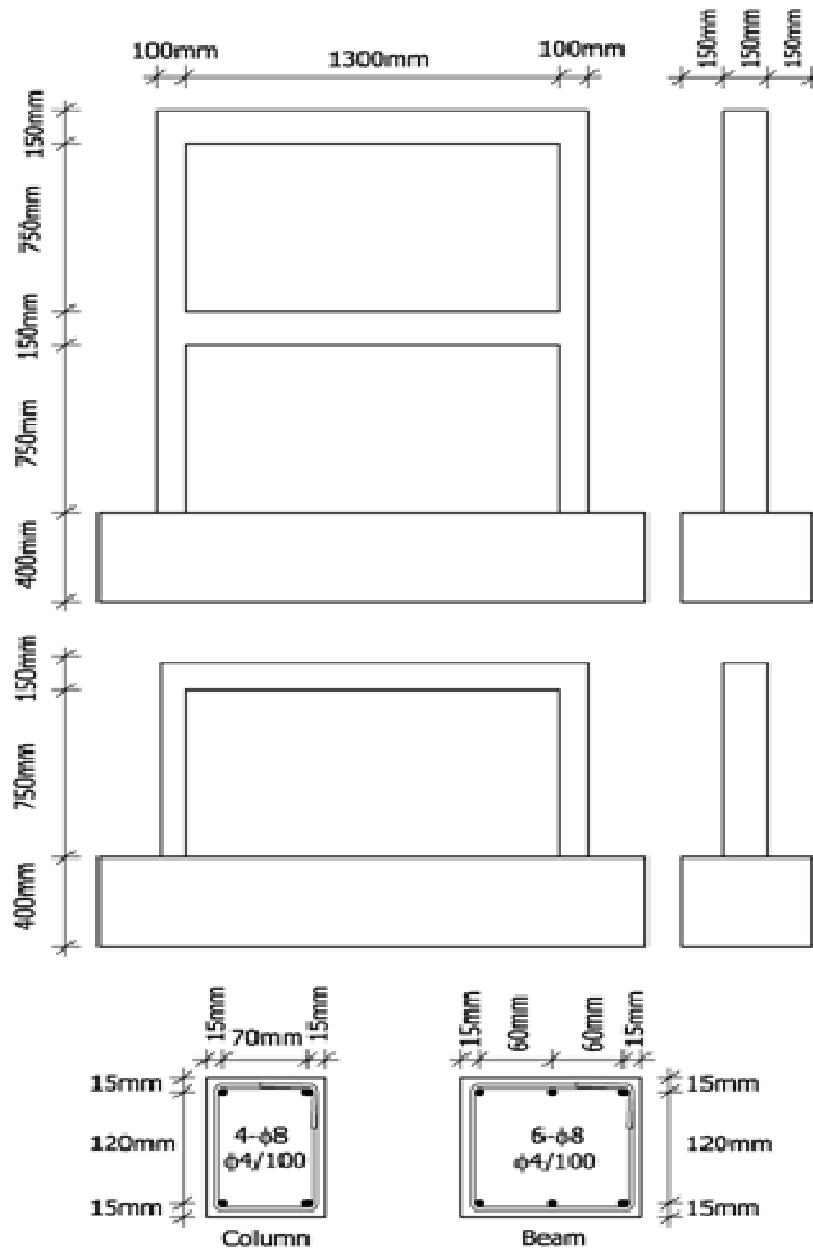


Figure 1. Dimensions and reinforcement of the test frames.

EXPERIMENTAL STUDIES

Test frames

In the experimental part of the study, one-third scale, one-bay, one and two-story RC frames were used as test units. Taking into account the fact that the building stock in Turkey and many countries around consists mainly of deficient RC framed buildings, test frames have intentionally been designed and constructed with the most common deficiencies observed in local practice, such as strong beam-weak column connections,

insufficient confinement, low-grade concrete, insufficient lap-splice length and poor workmanship. The frames had their columns fixed to the rigid foundation beams. Dimensions and reinforcement of both types of test frames are illustrated in Figure 1.

Materials

Low strength concrete was deliberately used in the test frames to represent the concrete commonly used in majority of existing buildings in Turkey. Both frame bays were infilled with scaled hollow

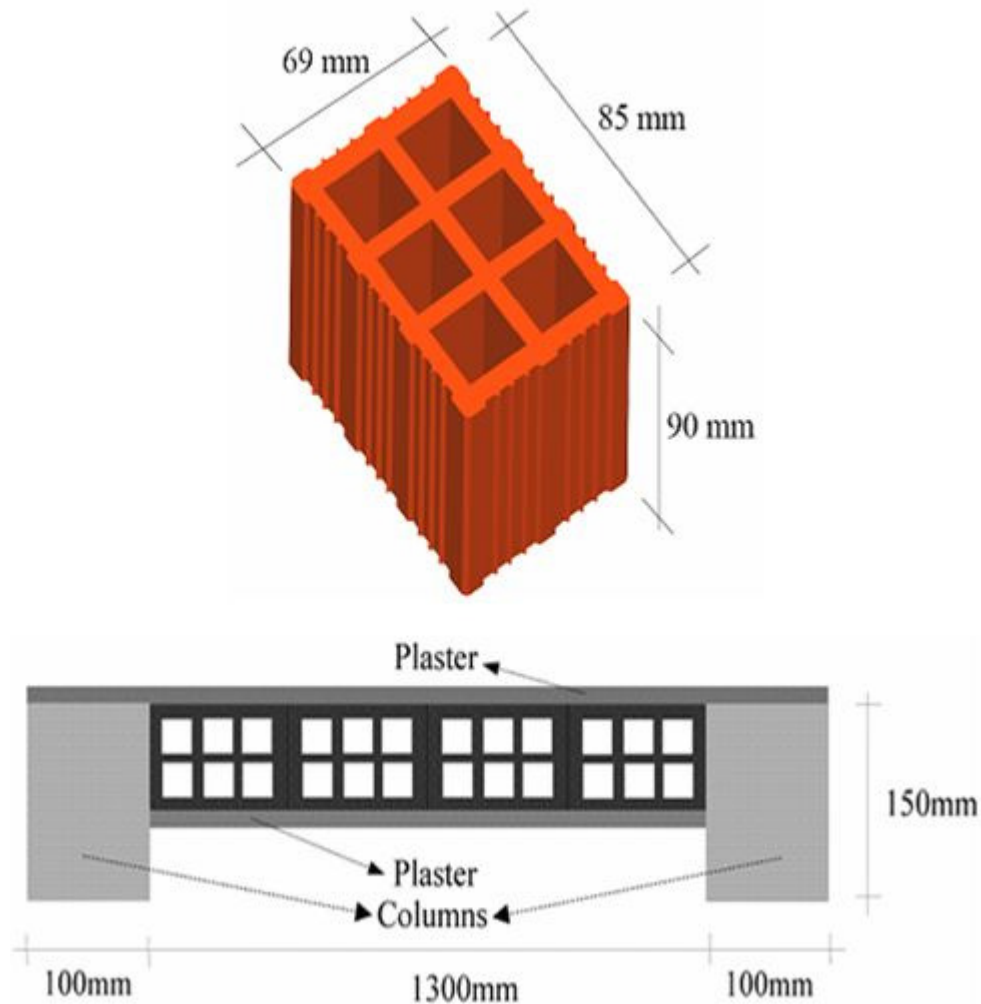


Figure 2. Hollow brick used as infill material and infilling method.

bricks (with void ratio of 0.52) covered with a scaled layer of plaster. Ordinary cement-lime mortar was used for the plaster, reflecting the usual practice. Hollow brick and infilling method is shown in Figure 2. Ordinary workmanship was intentionally employed in wall construction and plaster application. For the same reason, mild steel plain bars were used as longitudinal steel in both test frames. Typical properties of reinforcing bars used in this study and average compressive strength values for frame concrete and plaster determined on testing day are listed in Table 1.

Loading and supporting system

In Figure 3, general views of the test set-up for two and one-story test frames are given, respectively. As can be seen in Figure 3, tests were performed in front of a reaction wall. Frames were subjected to reversed cyclic lateral loading resembling seismic effects. The quasi-static test loading consisted of reversed cyclic lateral loading besides constant vertical load applied on both columns. The axial load on columns was provided by steel cables post-tensioned by hydraulic jacks.

Reversed cyclic lateral loading was applied by using a double acting hydraulic jack. The lateral loading system had pin

connections at both ends to eliminate any accidental eccentricity mainly in vertical direction and tolerating a small rotation in horizontal direction normal to testing plane. Lateral load was applied on a spreader beam at one-third of its span to ensure that the lateral load at second floor level always remains twice as the lateral load at first floor level. A very rigid external steel 'guide frame' attached to the universal base, was used to prevent any out-of-plane deformations. During the tests, increasing load cycles were applied up to the capacity of frame and beyond that, deformation controlled loading was performed with increasing displacement cycles. Load histories of all test frames are given in Figure 4.

Deformation measurement system

All deformations were measured by displacement transducers; using either linear variable differential transformers (LVDTs) or electronically recordable dial gages (DGs) as shown in Figure 3. Sway displacements were measured both at first and second floor levels. Infill wall shear deformations were determined on the basis of displacement measurements along the diagonals. Displacement measurements taken at the bottom of both columns were meant for computation of rotations of the entire frame. They also provided

Table 1. Material properties of test frames.

Test frame	Axial load N/N _o	No. of floors	Column steel	Lap-splice length	Long. Reinf. (MPa)	Trans. Reinf. (MPa)	Frame concrete (MPa)	Brick laying mortar (MPa)	Plaster (MPa)
SP1	0.11	2	Cont.	-	365	271	12.7	-	-
SP2	0.11	2	Cont.	-	365	271	13.3	3.4	-
SP3	0.11	2	Cont.	-	365	271	12.7	8.4	8.2
SP4	0.19	2	Cont.	-	330	220	16.6	6.5	6.5
SP5	0.30	2	Lapped	20 φ	330	220	8.6	3.5	3.5
SP6	0.10	2	Cont.	-	405	268	15.0	23.1 ⁽¹⁾	-
SP7	0.25	1	Cont.	-	330	220	15.6	6.1	6.1
SP8	0.13	1	Cont.	-	405	268	10.7	5.2	5.2
SP9	0.13	1	Lapped	20 φ	330	220	9.7	4.9	4.9

⁽¹⁾ Compressive Strength of RC Infil.

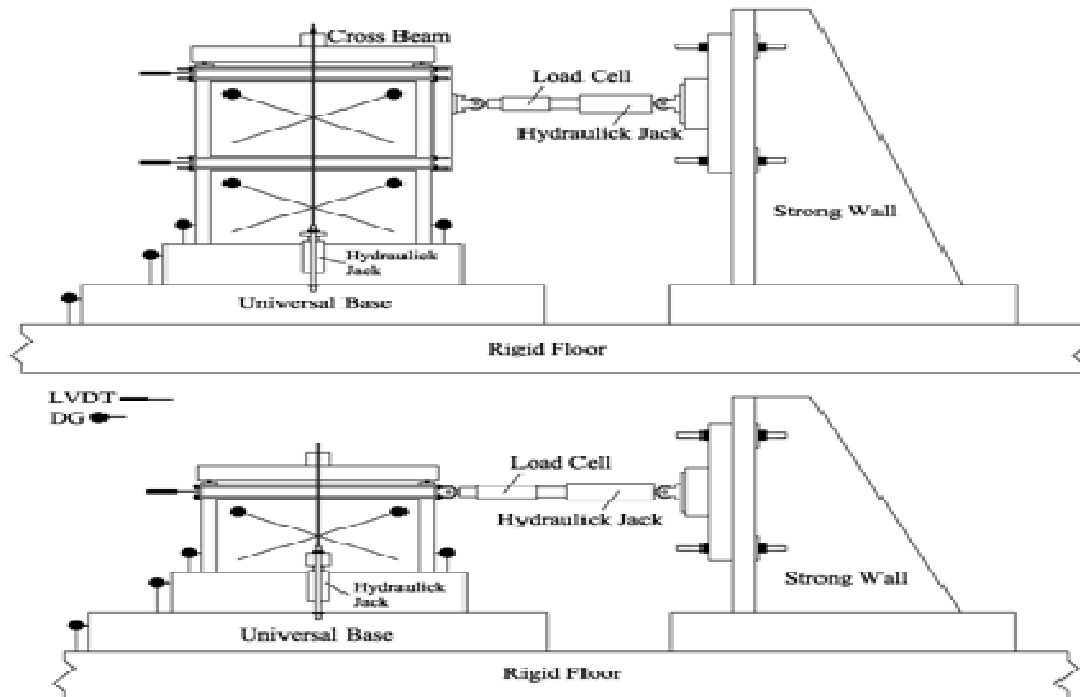


Figure 3. General view of test set-ups and deformation measurement systems.

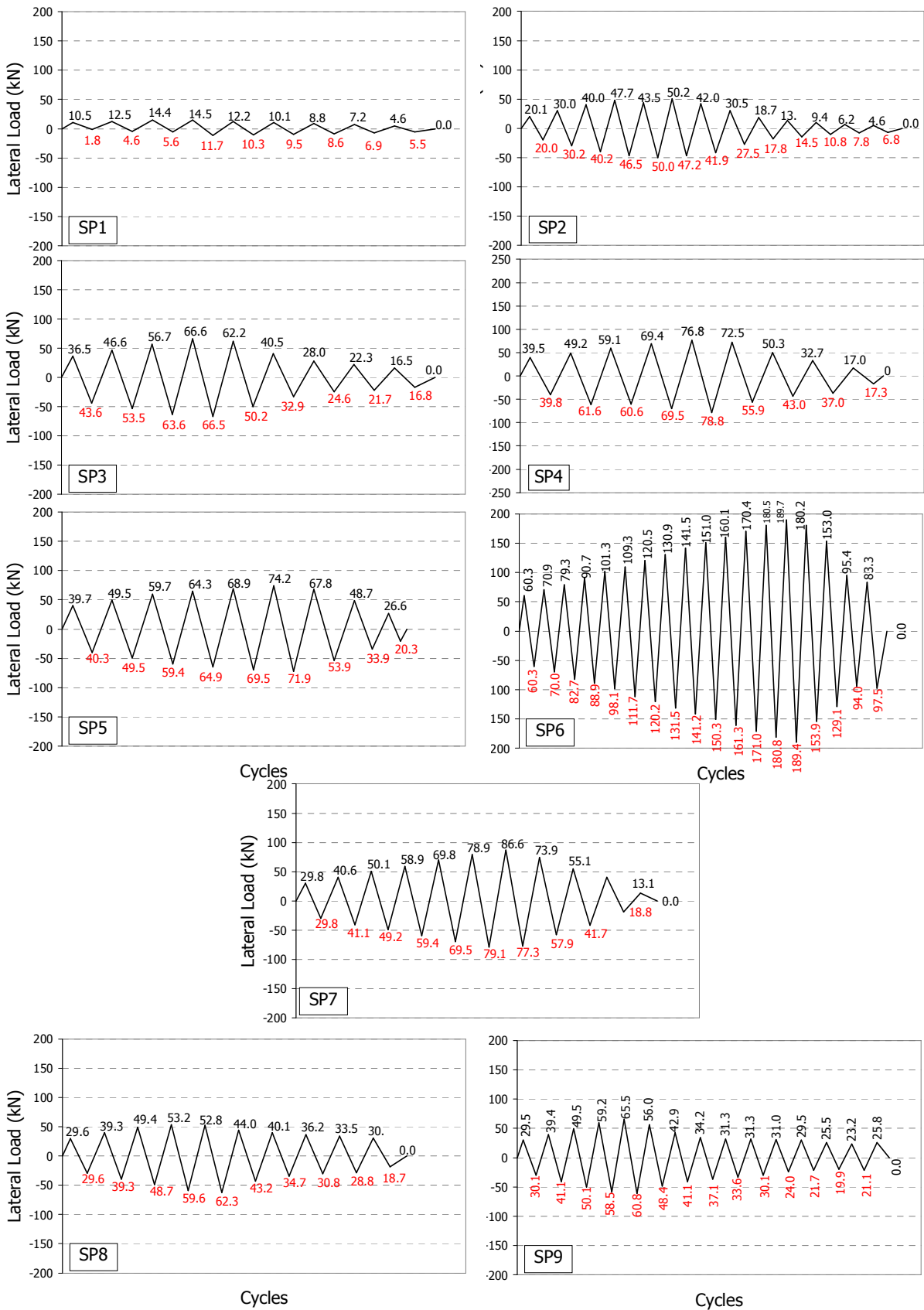


Figure 4. Load histories of all test frames.

Table 2. Performance indicators.

Test frame	Maximum lateral load (kN)	Ratio ⁽¹⁾	1st story drift ratio at peak δ_1/h	2nd story drift ratio at Peak $(\delta_2-\delta_1)/h$	Initial stiffness (kN/mm)	Energy dissipation (kJ)	Ductility
SP1	14.5	1.00	0.0160	0.0076	1.7	2.1	4.7
SP2	50.3	3.47	0.0113	0.0062	24.4	5.9	5.9
SP3	66.6	4.59	0.0043	0.0032	21.4	4.5	2.8
SP4	76.8	5.30	0.0042	0.0033	43.5	6.4	4.9
SP5	74.2	5.12	0.0035	0.0021	59.1	4.6	7.4
SP6	189.7	13.08	0.0079	0.0069	125.3	21.5	4.8
SP7	86.6	1.00	0.0036	-	95.8	5.7	10.0
SP8	62.3	0.72	0.0065	-	59.4	6.0	3.5
SP9	65.5	0.76	0.0053	-	59.9	8.6	5.3

⁽¹⁾ The ratio of Maximum lateral load to that of the reference frame.

data for monitoring the critical column section deformations; steel yielding in the tension side column, concrete crushing in the compression side column etc.

EXPERIMENTAL RESULTS

Behaviour of test specimens

One being bare and one hollow brick infilled (Sevil et al., 2010), one being RC infilled (Baran et al., 2009) and six plastered hollow brick infilled frames (Sevil., 2010; Baran and Tankut, 2009; Okuyucu and Tankut, 2009) were tested under vertical and quasi-static lateral loading simulating earthquake effect. Except from the bare and RC infilled, all frames exhibited typical masonry infilled frame behaviour characterized by: Rather rigid and linearly elastic behaviour at the initial stages, relatively high capacity resulting from infill wall contribution and rapid strength degradation and very rapid stiffness degradation upon infill wall crushing.

This expected behaviour was concluded by a typical failure accompanied by excessive permanent first story sway deformations. It is important to note here that although not plastered at both sides, test frame SP2 also exhibited typical masonry infilled frame behaviour. It was tested to observe effects of plaster application on infilled frame behaviour. Test frame SP6 was tested to observe

the RC infilled frame behaviour which forms an upper bound. As expected, this specimen behaved as a monolithic cantilever where failure took place at foundation level with column bases in terms of yielding of the steel in the tension side column and concrete crushing and buckling of longitudinal steel in the compression side column.

Test of SP5 Specimen was terminated since the diagonal crack just below the first story beam – left column joint turned out to be a shear failure and the column broke off due to low concrete strength of the frame. Story Drift Ratio is a term which is frequently used in the earthquake engineering as a measure of non-structural damage and to control second order effects. First and second story drift ratio values of the test frames at ultimate load levels are given in Table 2 and lateral load-first story drift ratio curves for the test frames are given in Figure 5. According to the story drift ratio curves, hollow brick infill walls and plastering increased lateral strength and stiffness. Bare test frame SP1 reached 1.60% lateral drift at ultimate load. This ratio was 1.13% for test frame SP2, with non-plastered hollow brick infills. As expected, test frames SP3, SP4 and SP5 with plastered hollow brick infills reached story drift ratios of 0.43, 0.42 and 0.35% values respectively.

Test frame SP6, with RC infills, had a drift ratio of 0.79% at its ultimate load which was lower than that of test frame SP1 but higher than masonry infilled specimens. As

expected, major damage took place in the first story infill wall for all two-story test frames. In addition, first story drift ratio values were higher than that of second story at ultimate load level for all test frames.

One-story test frames SP7, SP8 and SP9 had drift ratios of 0.36, 0.65 and 0.53%, respectively. The value for test frame SP7 was less when compared to the other two, since this frame had continuous column longitudinal bars together with higher axial column loads. Drift ratios were 0.42 and 0.43% for the test frames SP4 and SP3, which were the equivalent pairs for test frames SP7 and SP8, having drift ratios of 0.36 and 0.65% respectively. Equivalent pairs had all the variables same except the number of stories that test frames had. As expected, first story drift ratio value for test frame SP3 was greater than that of test frame SP4 and value for test frame SP8 was greater than that of test frame SP7 since higher axial load made the infills and frames much stiffer.

According to the Turkish Seismic Code (2006), maximum story drift index is limited to 0.0035 in the elastic analysis of the structure whereas, it is specified as 0.010 for inelastic analysis. On the other hand, according to clause 1630.10 of UBC (Uniform Building Code, 1997), the maximum story drift index is limited to 0.025 for the structures with a fundamental period less than 0.7 s and 0.020 for the structures with a fundamental period greater than 0.7 s. Hollow brick infilling reduces the amount of deformations as compared to bare test frame SP1.

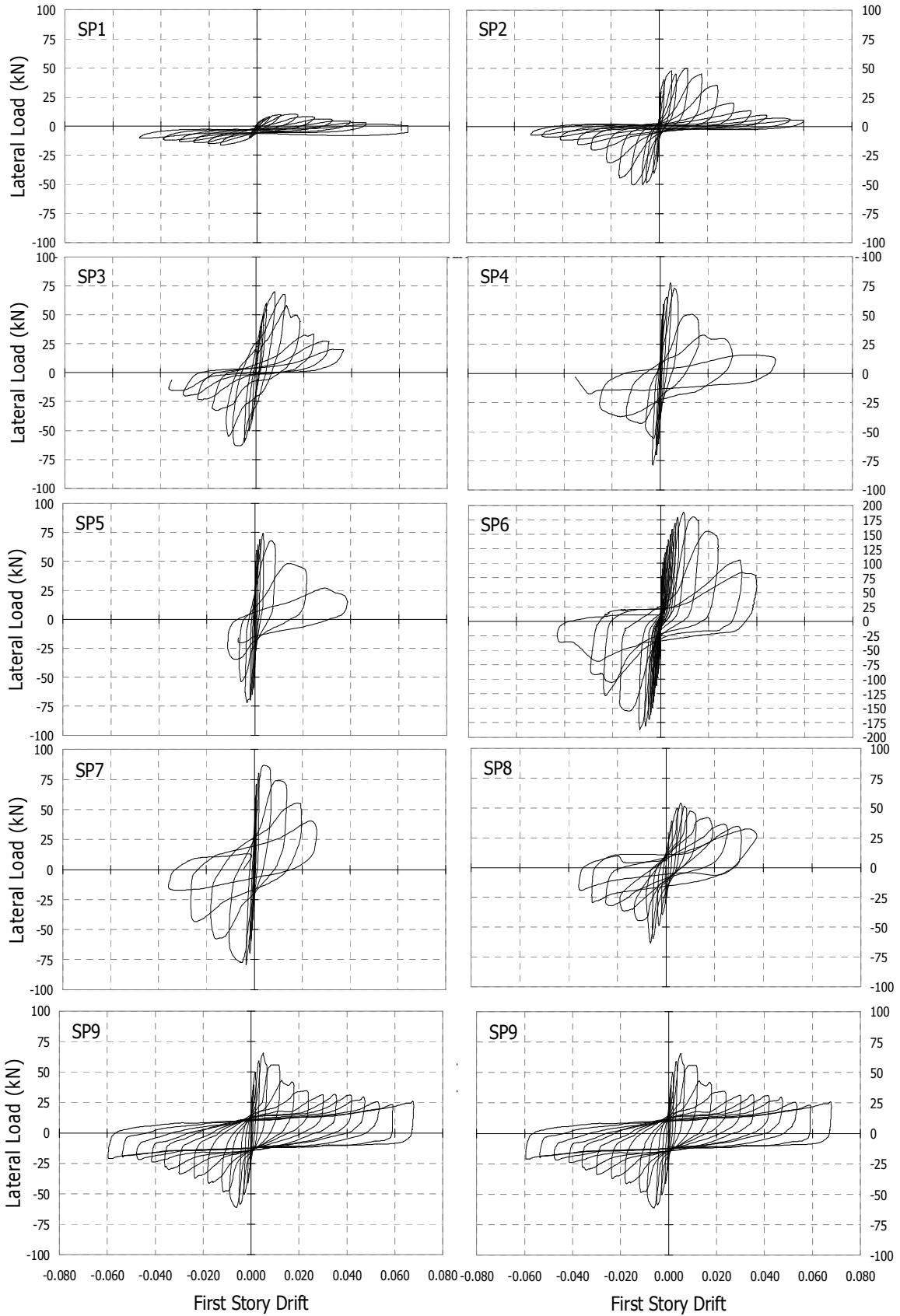


Figure 5. Lateral load-first story drift curves.

DISCUSSION OF TEST RESULTS

Strength and stiffness

Test frame performances are evaluated in terms of load-top displacement, energy dissipation and initial stiffness values as summarized in Table 2. When the results in Table 2 are examined, it can clearly be observed that there was no significant difference between the lateral load capacities of test frames SP4 and SP5 although one of them had continuous longitudinal bars through the height of the specimen whereas the other had lap splices at both floor levels with a length of 20ϕ (160 mm). This situation was owing to the level of the axial load applied on to the columns during the experiments of these two specimens. Total axial load on both columns was approximately 117.7 kN during the experiments of both specimens. This load level corresponded to 20% of the column's axial load capacity, which can be considered as high. With the application of relatively higher axial load level on both columns of test frame SP5, the lap splice effect could not be observed at a lateral load level of approximately 75 kN which was the lateral load capacity of both test frames. However, when total axial load on both columns is 10% of the column's axial load capacity, lateral load capacity of the frame decreased to 65 kN level, as in the case of test frame SP3. It should be noted that lateral load capacity of test frame SP3 is less than that of test frame SP5 although there were no lap-splices in test frame SP3 but had lower axial load on its columns. This situation shows the importance of the column's axial load level on the strength of the RC test frame. In addition, the decrease is more pronounced in the case of one story test frames.

Test frame SP2 had non-plastered hollow brick infills in contrast to test frames SP3, SP4 and SP5. As expected, this specimen had lower lateral strength (about 50 kN) as compared to SP3, SP4 and SP5. The ratio of strength increase as compared test frame SP1 was almost 3.5 times of test frame SP2, where this value was approximately 5.0 times for test frames SP3, SP4 and SP5. This shows the importance of the effect of hollow brick infilling on the RC frame behaviour, although it was non-plastered. In addition, plastering the hollow bricks obviously enhances the strength increase that is supplied only by hollow brick infilling. However, non-plastered hollow brick infilled frame SP2 showed more ductile behaviour than the plastered brick infilled frame. This can be attributed to the fact of higher stiffness of plaster than masonry. Test frames SP4 and SP3 had maximum lateral loads of 78.8 and 66.6 kN, respectively. These values were 86.6 and 62.3 kN for the respective equivalent pairs of one-story test frames.

Strength and stiffness characteristics together with the general behaviour of specimens were evaluated by the help of response-envelope curves shown in Figure 6, which were constructed by connecting the peak points of

the hysteretic load-displacement curves of the test frames for each forward and backward cycle. For two-story specimens, second story level displacements were used. However, in order to be able to make a comparison; first story level displacements were used in the comparison of all test frames. These curves indicate that hollow brick infills significantly increase strength and stiffness and improve ductility of frames. The photographs of all specimens after failure are given in Figure 7.

The initial stiffness of a specimen was calculated by using the slope of the linear part of the first forward load excursion (Baran, 2005). It was used as a relative indicator in improvement of the rigidities of test frames. As it can be seen in Table 2, hollow brick infills increased initial stiffness of specimens significantly. The increase was nearly 20 times for two story hollow brick infilled test frames and approximately 30 times for one story test frames. The variation in the initial stiffness values for the two groups can be owing to the number of stories. It should be noted that quality of the workmanship in the construction of the hollow brick infill wall and plastering of the specimen played an important role in the displacement history in early cycles.

Energy dissipation capacities

Energy dissipation capacity is an important indicator of the structure's ability to withstand severe ground motions. Energy dissipation capacity (Baran, 2005) is an important indicator of the improved behaviour. For specimens, the amount of dissipated energy was determined by calculating and adding the areas under the lateral load - hydraulic jack level displacement curves for each cycle. For one-story test frames, hydraulic jack is at the level of first story beam which means that lateral load-top displacement graphs were used for energy dissipation calculations. It is important to note here that the energy dissipation characteristics of the test frames strongly depends on the loading history. The loading histories of the test frames were intended to be the same, but when the response of a test frame became non-linear, backward and forward half cycle loadings were controlled by top story level displacements. The same top story level displacements were intended to be reached for the forward and backward half cycles. Total amount of dissipated energy of each specimen is tabulated in Table 2. As it can be seen in this table, that hollow brick infilling improve the energy dissipation characteristics of the test frames.

Ductility

Displacement ductility is defined by the ratio of the ultimate displacement to yield displacement. The

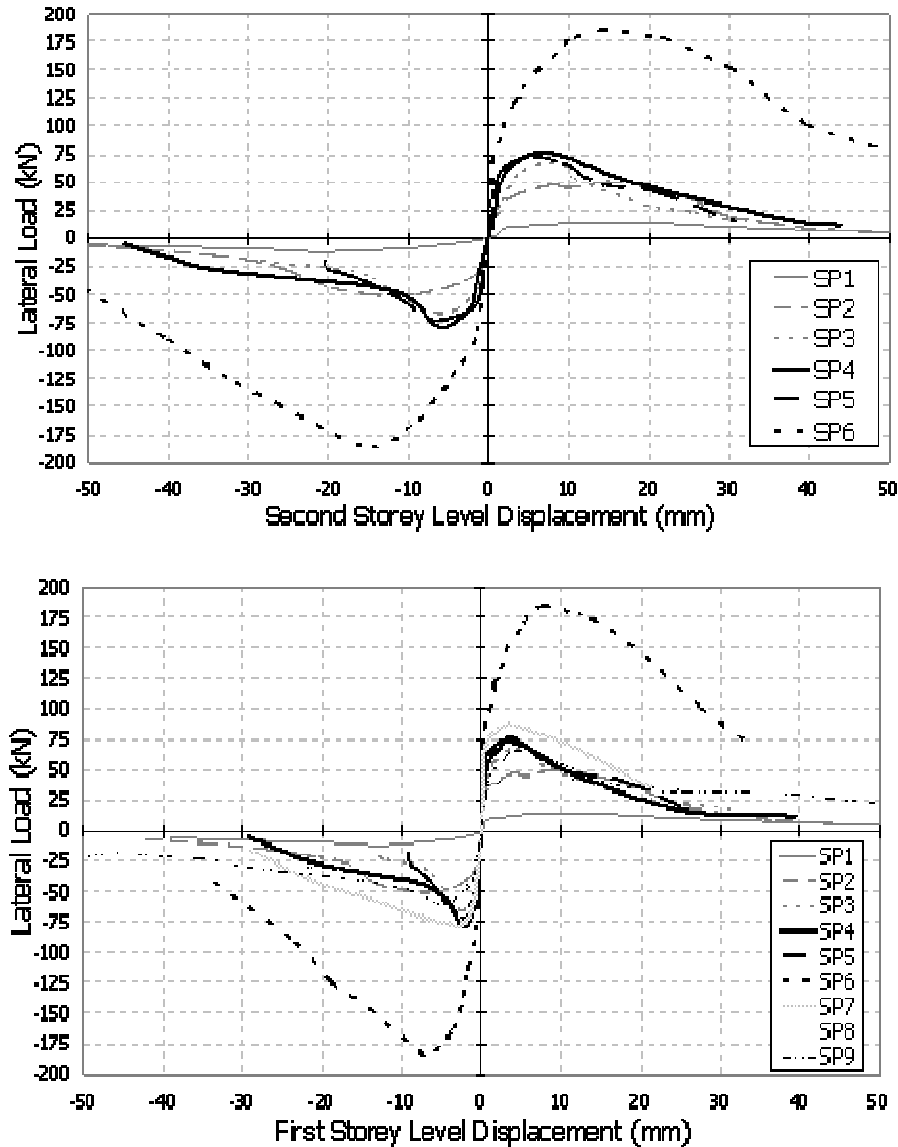


Figure 6. Envelope load-displacement curves (for two-story and one-story test frames).

ultimate displacement is defined as the top story level displacement at which the lateral load dropped to 85% of the maximum applied load at post peak region. The yield displacement was described with a secant drawn starting from the origin and passing from the point on which lateral load is 70% of the maximum applied load. This secant line was extended up to the horizontal line drawn from the maximum load and corresponding displacement was accepted as yield displacement (Sezen and Moehle, 2004; Sevil, 2010). The calculated ductility values are listed in Table 2. As it can be observed, one-story test frames SP7 and SP8 showed more ductile behaviour than equivalent two-story test frames SP4 and SP3, respectively. In addition, two-story test frame SP4 and one-story test frame SP7, which had higher column axial

loads (nearly 25% of column axial load capacity) showed more ductile behaviour than two-story test frame SP3 and one-story test frame SP8, respectively which had lower column axial loads (nearly 10% of column axial load capacity). This situation can be owing to the more dominant compressive and shear stresses in one-story frames and more efficient behaviour of the infill, which can be positively influenced by the confining effect of compressive forces. Although test frame SP5 had two-stories, it showed more ductile behaviour than one-story test frame SP9 which had lower column axial load. It should be noted here that, test frame SP2, which had non-plastered hollow bricks, showed more ductile behaviour than bare test frame SP1 and RC infilled test frame SP6.



Figure 7. Test frames after failure.

ANALYTICAL STUDIES

Infill wall modeling

Beginning with the first study conducted by Polyakov (1957), analytical and experimental studies on infills have

been conducted for nearly fifty years. During his studies, Polyakov observed diagonal cracks in the center region of the infill, separation over a finite length of the beam and the column between the frame member and the infill at the unloaded corners and full contact between them adjacent to two opposite loaded corners. In the 1960's,

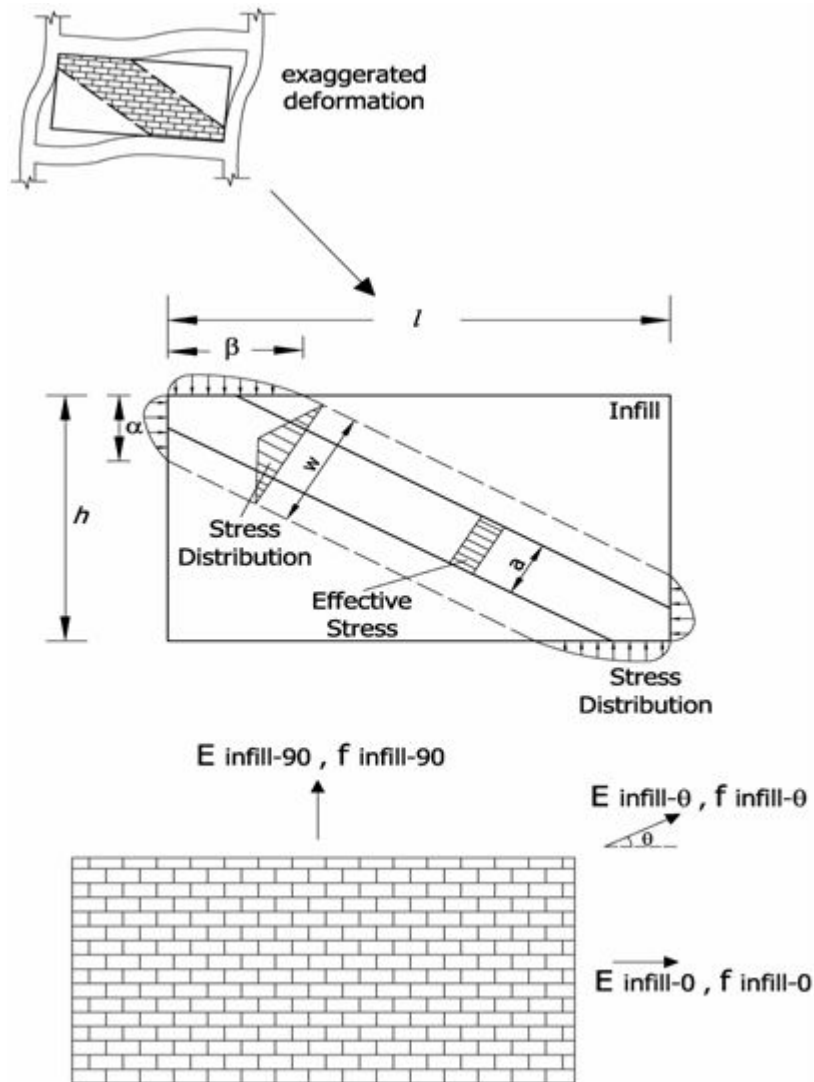


Figure 8. Equivalent diagonal compression strut replacing infill and orthotropic model for infill.

Smith (1962, 1966, 1967, 1968) and Smith and Carter (1969) modeled the infill walls as equivalent diagonal compression struts. In the 1970's (Mainstone and Weeks, 1970; Mainstone, 1974; Klingner and Bertero, 1978) in the 1990's (Paulay and Priestley, 1992; Angel et al., 1994; Saneinejad and Hobbs, 1995) and in the early 2000's (Al-Chaar, 2002; El-Dakhkhni et al., 2003) conducted analytical and experimental studies on the infill walls and contribute to better understanding of the infilled frame behaviour. Results obtained by Smith and Carter (1969) showed similarity to experimental results obtained by Mainstone (1974) and Al-Chaar (2002).

In their studies, Smith and Carter (1969) assumed that the frame and the infill are not bonded together. When the load is applied, the frame and the infill separates over a finite length of the beam and the column and the

contact between them remains adjacent to two opposite corners. At this stage, a line drawn from one loaded corner to the other represents the direction of the principal compression. Therefore, the panel transfers compression along this line. In fact, it can be assumed that the infill behaves as a diagonal strut and the structure can be analyzed with equivalent struts replacing the infills, as shown in Figure 8. A diagonal compression strut can adequately represent load transfer mechanism observed from the experiments and conducted finite element analysis. Here α and β are the interaction distribution parameters as presented in Figure 8. In the case of infills with masonry materials, Equations 1 and 2 are proposed by FEMA (1998) for the determination of the mechanical and the geometrical properties of the equivalent diagonal strut;

$$a_{infill} = 0.175(\lambda \cdot h_{col})^{-0.4} d \tag{1}$$

$$\lambda = \sqrt[4]{\frac{E_{infill} b_w \sin(2\beta_s)}{4E I h_{inf}}} \tag{2}$$

where a_{infill} is the effective width of the equivalent diagonal strut, λ is a dimensionless parameter, h_{col} is the column height between centerlines of beams, d is the diagonal length of infill panel, E_{inf} is Young’s modulus of the infill, b_w is the thickness of the infill, β_s is the angle whose tangent is infill height to length, E is Young’s modulus of the column, I is the moment of inertia of the column and h_{inf} is the height of the infill.

The equivalent compression strut shall have the same thickness as the infill it represents.

In the analytical studies conducted, plastered hollow brick infill walls were modeled by equivalent diagonal compression struts. Therefore, axial strength (f_{cm}) and stiffness of the struts should be computed. The axial strength (f_{cm}) and stiffness of the struts can be obtained from the tests of square plastered hollow brick infill panels under diagonal compression. However, in the absence of the panel tests, Equations 3 and 4 proposed by Binici and Ozcebe (2006), can be used to predict the strength and stiffness of the plastered hollow brick infill in vertical direction;

$$f_{infill90} = \frac{(f_{brick} \cdot t_{brick} + f_{plaster} \cdot t_{plaster})}{(t_{brick} + t_{plaster})} \tag{3}$$

$$E_{infill90} = \frac{(E_{brick} \cdot t_{brick} + E_{plaster} \cdot t_{plaster})}{(t_{brick} + t_{plaster})} \tag{4}$$

E_{brick} is the Young’s modulus of the infill material.

Binici and Ozcebe (2006) proposed its value to be varying between 500 to 1500 times the compressive strength of the infill. Hollow bricks used in the infills of the test frames were loaded in the direction of (Duvarci, 2003) and perpendicular to the holes and the results are given in Table 3.

Since the infill is diagonally compressed when the infilled frame is loaded laterally, El-Dakhakhni et al. (2003) made a justifiable assumption that the properties in the diagonal direction are the governing material properties. Plastered hollow brick infills are anisotropic. At this point, another assumption is made by considering the anisotropic infill as orthotropic. Since the infill of the test frames behave as it is under compression, Equation 5 derived by using constitutive relations of orthotropic plates and axes transformation matrix, can be used to

obtain the Young’s modulus of the infill in the diagonal direction, $E_{infill-\theta}$;

$$E_{infill-\theta} = \frac{1}{\frac{1}{E_{infill0}} \cos^4\theta + \left[\frac{2\nu_{0-90}}{E_{infill0}} + \frac{1}{G} \right] \cos^2\theta \cdot \sin^2\theta + \frac{1}{E_{infill90}} \sin^4\theta} \tag{5}$$

$E_{infill-0}$ and $E_{infill-90}$ are Young’s modulus of the infill in the direction parallel to and normal to mortar bed joints respectively, ν_{0-90} is Poisson’s ratio defined as the ratio of the strain in the direction normal to the mortar bed joints to the strain in the direction parallel to the mortar bed joints. ν_{0-90} can be taken as 0.25 and $E_{infill-0}$ as half of $E_{infill-90}$. G is shear modulus.

The use of Equation 5 for unreinforced concrete infill walls reduces Young’s modulus in the inclined direction to about 75% of that in the direction perpendicular to the mortar bed joints. Although depending mostly upon the hollow brick’s void ratio, an average ratio of 70% can be taken as for the case of plastered hollow brick infills. Initial Young’s modulus is commonly related to ultimate compressive strength of concrete or masonry like materials. It would be a justifiable assumption that not only Young’s modulus, but also the ultimate strength of the infill in the θ direction, $f_{infill-\theta}$, also changes. A simplification can be made at this point for taking into account the variation in direction by using a smaller factor relating $E_{infill-\theta}$ to $f_{infill-\theta}$ and $E_{infill-90}$ to $f_{infill-90}$, since the infill wall is anisotropic. The assumption that compressive strength of the infill varies according to the angle of loading was investigated by Hamid and Drysdale (1980) and a value of $f_{infill-\theta} = 0.7f_{infill-90}$ was suggested by Seah (1998). The orthotropic model for the infill given by El-Dakhakhni et al. (2003) is illustrated in Figure 8. Nonlinear finite element analysis conducted by Saneinejad and Hobbs (1995) suggested that the secant stiffness of the infilled frames at the peak load to be half the initial stiffness. This suggestion might be adapted to the calculation of the Young’s modulus at peak load, $E_{infill-p} = 0.5E_{infill-\theta}$.

A trilinear relation stress-strain diagram for concrete masonry infill is suggested by El-Dakhakhni et al. (2003) instead of the parabolic one as shown in Figure 9. Accordingly, this approximation is simpler and more practical for analysis. Accepting the strain ϵ_2 equal to the strain ϵ_1 , using an average value of $E_{infill-0}$ and $E_{infill-90}$ for modulus of elasticity and accepting $f_{infill-\theta} = 0.6f_{infill-90}$ yield satisfactory estimations for the deformation capacity of the equivalent compression strut. Hence, a stress-strain diagram as shown in Figure 10 for the equivalent compression strut modeling the plastered hollow brick infill wall, was used in the analytical studies. Test results showed that axial load applied on the frames increased the push over capacity of the specimens. Therefore, axial load should have effect on the ultimate load carrying

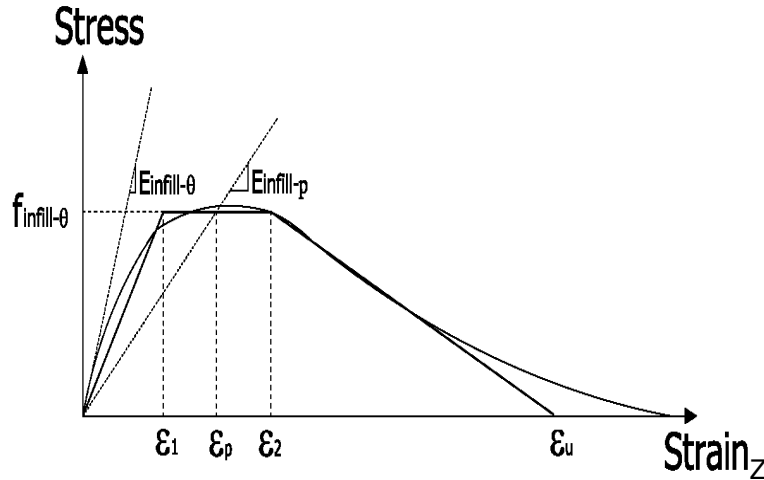


Figure 9. Simplified stress-strain diagram of concrete.

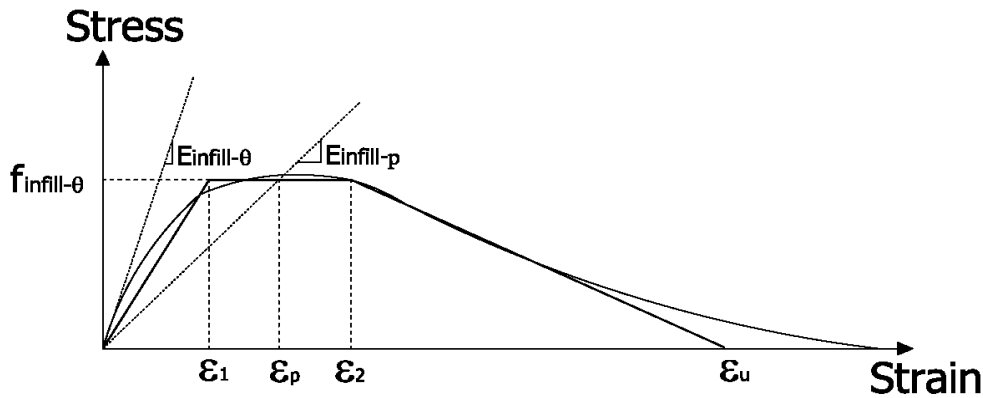


Figure 10. Stress-strain diagram for the compression strut modeling plastered hollow brick infill.

capacity of the strut and should be taken into account. The ultimate load carrying capacity and the yield deformation of the strut were calculated by using Equation (6)

$$F = \gamma \cdot f_{infill-\theta} \cdot a_{infill} \cdot b_w = \gamma \cdot f_{cm} \cdot a_{infill} \cdot b_w \quad (6)$$

In Equation (6) γ is a variable due to column axial load effect on the ultimate load carrying capacity of the strut. When test results are analyzed, adjusting γ as in Equation (7) seems to be a practical and safe assumption;

$$\gamma = 1 + \left(\frac{N}{N_0} \right) \leq 1.3 \quad (7)$$

An upper level of 1.3 for γ is proposed since a maximum axial load of approximately 58.8 kN corresponding to

30% of column's axial load capacity was applied during the tests. Taking the ultimate strain of the equivalent compression strut as $\epsilon_u = 0.018$ yields satisfactory results in analytical studies.

Lapped-splice strength

In case of test frames with lapped-splices on column steels, the yield stress could not be reached at some regions due to insufficient lapped-splice lengths at floor levels. At the joints, the yield stress was decreased proportional to the splice length of the longitudinal steel and interaction curves of these sections were calculated by using reduced yield stresses. For these test frames, it was intended to compute the column capacities by using the actual lapped-splice strengths. It is known that nearly the full yield stress of longitudinal steel can be used in the calculations when the lapped-splice length is not less than 40ϕ . Hence, yield stress of the longitudinal steel, f_y ,

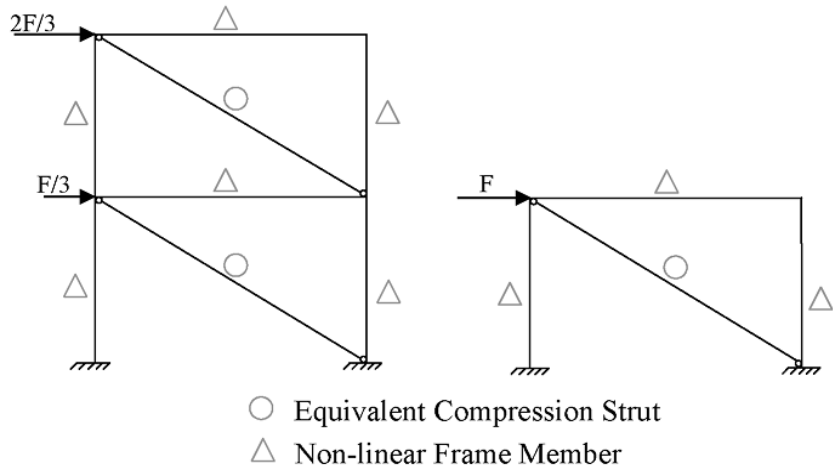
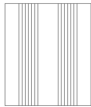
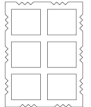


Figure 11. Analytical model of the test frames.

Table 3. Results of compression tests of tiles (MPa).

Tile no.	Failure load (kN)	Compressive strength (Net area)	Compressive strength (Gross area)
	49.87	17.71	8.50
	17.18	10.05	2.77

can be decreased proportional to the square root of lapped-splice length of the steel. Since the lapped-splice length at the floor levels were 20ϕ , the reduced yield stress of the longitudinal steel, f'_y can be calculated using Equation (9) given by Canbay and Frosch (2005):

$$f'_y \cong f_y \cdot \sqrt{\frac{20\phi}{40\phi}} = 0.7071 \cdot f_y \tag{8}$$

Push-over analysis

Push-over curves of the test frames were drawn to be able to compare the experimental results with those obtained from analytical studies conducted. Push-over analysis is a kind of nonlinear static analysis procedure that is generally used to evaluate the performance of the

structures under lateral loads. In the push-over analysis, a load pattern is selected first and applied to the structure in incremental steps. The computer program accepts axial load-moment interaction curve or just yield moment values of the members. In the present study, interaction curves were used for columns whereas just yield moment values were used for the beams idealizing beam behaviour as elasto-plastic. Lapped-splices in the column longitudinal steels (if exist) were taken into account. Analytical model of the test frames is given in Figure 11. It is assumed that the equivalent compression struts were hinge-connected to the frames at both ends.

COMPARISON OF ANALYTICAL AND EXPERIMENTAL RESULTS

As it can be seen in Figures 12, 13 and Table 4,

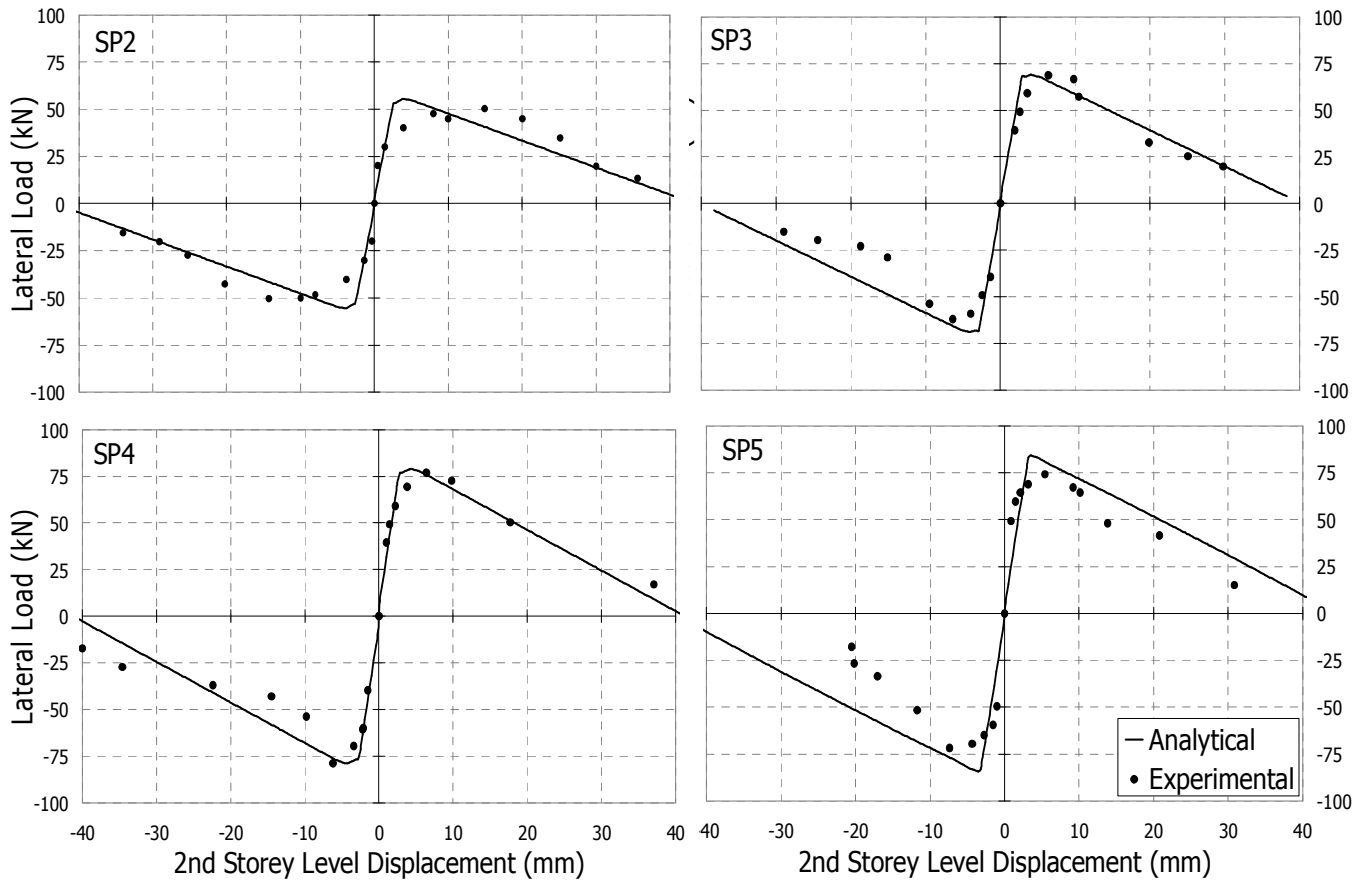


Figure 12. Comparison of analytical and experimental load-displacement curves (two-story).

push-over analysis (Baran et al., 2010) made by the proposed analytical method, where plastered hollow brick infills modeled by equivalent diagonal compression struts, gave safe and sound results in estimating the ultimate load capacities of the test frames. With the proposed method, the deviation in the estimation of the ultimate load carrying capacities of the test frames stated in \pm about 10% range of the experimental values. In addition, post-peak portions (descending portions) of the push-over curves were adequately simulated by the proposed method. However, initial stiffness values of the infilled test frames could not be estimated within acceptable closeness for all test frames. This can be owing to the quality of the workmanship in the hollow brick infill wall and plastering of the specimen which played an important role in the displacement history in early cycles. Since the proposed method is for hollow brick infilled RC frames, push-over analysis for bare test frame SP1 and RC infilled test frame SP6 were not conducted.

Conclusions

The conclusions presented below are based on the

limited data obtained from tests of RC frames and analytical studies conducted. The plastered hollow brick infills, used as partition walls, increased both strength and stiffness of frames. In the test of frames with masonry infills, the increase in strength was nearly 6 times as compared to the bare frame for both frame types. This increase in initial stiffness was nearly 20 and 30 times for two and one-story test frames, respectively. For RC infilled frame, the increase in strength and initial stiffness was nearly 15 and 60 times as compared to the bare frame. This proved the effectiveness of the method in improving the overall seismic structural performance.

Application of plaster on both sides of the hollow brick infill increased lateral load carrying capacity of the frame. The increase was nearly 3.5 times as compared to the bare frame. For both types of frame, one of the main difference is the application level of loading. In two-story frames, the lateral load was applied at a greater height and therefore moment arm is greater resulting in more overturning effect. Therefore, more tensile stress occurs at the tension side column of two-story frames. However, compressive and shear stresses are more dominant in one-story frames. This is the most possible reason for higher initial stiffness of one-story frames.

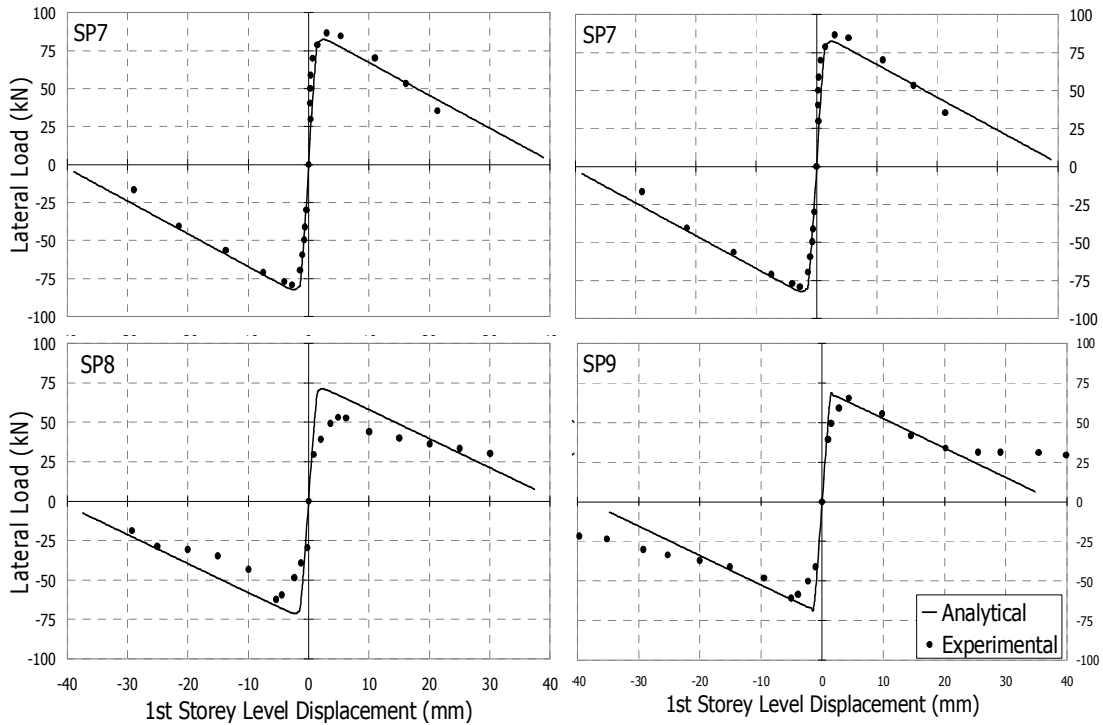


Figure 13. Comparison of analytical and experimental load-displacement curves (one-story).

Table 4. Comparison of experimental response curves with the analytical push-over curves.

Specimen	Ultimate load (kN)			Initial stiffness (kN/mm)		
	Experimental	Analytical	Ratio ⁽¹⁾	Experimental	Analytical	Ratio ⁽¹⁾
SP2	50.3	55.4	0.91	24.4	31.0	0.79
SP3	66.6	69.0	0.97	21.4	31.9	0.67
SP4	76.8	79.0	0.97	43.5	58.4	0.74
SP5	74.2	84.2	0.88	59.1	39.8	1.48
SP7	86.6	82.3	1.05	95.8	77.3	1.24
SP8	62.3	71.4	0.87	59.4	56.8	1.05
SP9	65.5	68.7	0.95	59.9	57.5	1.04

⁽¹⁾Ratio of the experimental data to the analytical data.

Two-story and one-story equivalent test frames showed very similar behaviour, especially lateral load capacities of equivalent pairs were close. Presence of inadequate (20 bar diameter) lapped-splices on column longitudinal steels did not seem to adversely affect the infill effectiveness significantly, if the column axial load was not less than 20% of its axial load capacity. Hence, bond problems due to lapped-splices on column steels would not be critical in the cases when the axial load level on the columns are not very low. Independent from the presence of lapped-splice in steel, lower axial load on columns created a negative effect on the lateral strength. Hence, it can be concluded that higher column axial loads made the infills stronger which provided higher

lateral load capacity to the frame. This phenomenon was taken into account in calculating the ultimate load carrying capacity of a compression strut modeling the plastered hollow brick infill.

The proposed equivalent diagonal compression strut modeling showed good correlation with the test results. In the structural design process, equivalent diagonal compression struts modeling the plastered hollow brick infills can easily be added to the existing frame model of the buildings. By this way, considerable amount of time and work might be saved by the use of this method which enables the quick determination of the ultimate load carrying capacities of the frames with plastered hollow brick infills.

List of symbols

ϕ	: Reinforcing bar diameter
β_s	: Angle whose tangent is infill height to length
δ	: Relative displacement between two successive floors
ϵ	: Strain
γ	: A variable due to column axial load effect on the ultimate load carrying capacity of the strut
λ	: A dimensionless parameter
μ_{0-90}	: Poisson's ratio defined as the ratio of the strain in the direction normal to the mortar bed joints to the strain in the direction parallel to the mortar bed joints
ϵ_u	: Ultimate strain of the equivalent compression strut
a_{infill}	: Effective width of the equivalent diagonal strut
b_w	: Thickness of the infill
d	: Diagonal length of infill panel
E	: Young's Modulus of the column
E_{brick}	: Young's modulus of the infill material
E_{inf}	: Young's Modulus of the infill
$E_{infill-p}$: Young's modulus at peak load
$E_{infill-0}$: Young's modulus of the infill in the direction parallel to mortar bed joints
$E_{infill-90}$: Young's modulus of the infill in the direction normal to mortar bed joints
$E_{infill-\theta}$: Young's modulus of the infill in the θ direction
$E_{plaster}$: Young's modulus of the plaster
F	: Ultimate load carrying capacity
f_{brick}	: Ultimate strength of the infill material
f_{cm}	: Axial strength
$f_{infill-0}$: Ultimate strength of the infill in the direction parallel to mortar bed joints
$f_{infill-90}$: Ultimate strength of the infill in the direction normal to mortar bed joints
$f_{infill-\theta}$: Ultimate strength of the infill in the θ direction
$f_{plaster}$: Ultimate strength of the plaster
f_y	: Yield stress of the longitudinal steel
f_y'	: Reduced yield stress of the longitudinal steel
G	: Shear modulus
h	: Story height
h_{col}	: Column height between centerlines of beams
h_{inf}	: Height of the infill
I	: Moment of inertia of the column
N/N_o	: Column axial load level
t_{brick}	: Thickness of the infill material
$t_{plaster}$: Thickness of the plaster

REFERENCES

- Al-Chaar G (2002). Evaluating Strength and Stiffness of Unreinforced Masonry Infill Structures. Construction Engineering Research Laboratory, January.
- Angel R, Abrams DP, Shapiro D, Uzarski J, Webster M (1994). Behaviour of Reinforced Concrete Frames with Masonry Infills. Structural Research Series No.589, University of Illinois at Urbana-Champaign, UILU ENG 94-2005: 183.
- Baran M (2005). Precast Concrete Panel Reinforced Infill Walls for Seismic Strengthening of Reinforced Concrete Framed Structures. Ph D Thesis, Middle East Technical University, Ankara, Turkey.
- Baran M, Okuyucu D, Tankut T (2009). Seismic Strengthening of R/C Framed Structures by Precast Concrete Panels (Experimental Studies) (in Turkish). Int. J. Eng. Res. Dev., 1(1): 63-68.
- Baran M, Tankut T (2009). Effect of Lapped Splice Deficiency on Behaviour of R/C Frames (in Turkish). Int. J. Eng. Res. Development, 1(2): 71-75.
- Baran M, Canbay E, Tankut T (2010). Seismic Strengthening with Precast Concrete Panels – Theoretical Approach (in Turkish). UCTEA, Turkish Chamber of Civil Engineers, Tech. J., 21(1): 4959-4978.
- Binici B, Özcebe G (2006). Seismic Evaluation of Infilled Reinforced Concrete Frames Strengthened with FRPS. Proceedings of the 8th U. S. National Conference on Earthquake Engineering. San Francisco, California, USA, Paper No. 1717.
- Canbay E, Frosch RJ, (2005). Bond Strength of Lapped-Spliced Bars. ACI Structural Journal, July-August 2005, Title no: 102-S62.
- Duvarci M (2003). Seismic Strengthening of Reinforced Concrete Frames with Precast Concrete Panels. MS Thesis, Middle East

- Technical University, Ankara, Turkey.
- El-Dakhkhni WW, Elgaaly M, Hamid AA (2003). Three-Strut Model for Concrete Masonry-Infilled Steel Frames. *J. Struct. Eng.*, pp. 177-185, February.
- Federal Emergency Management Agency (FEMA) (1998). Evaluation of Earthquake Damaged Concrete and Masonry Wall Buildings, FEMA 306.
- Hamid AA, Drysdale RG (1980). Concrete Masonry under Combined Shear and Compression Along the Mortar Joints. *ACI J.*, 77: 314-320.
- Kaplan SA (2008). Dolgu Duvarların Betonarme Taşıyıcı Sistem Performansına Etkisi. *Türkiye Mühendislik Haberleri*, 452-2008/6.
- Klingner RE, Bertero V (1978). Earthquake Resistance of Infilled Frames. *J. Struct. Division ASCE*, 104, June.
- Mainstone RJ, Weeks GA (1970). The Influence of Bounding Frame on the Racking Stiffness and Strength of Brick Walls. 2nd International BrickMasonry Conference held at Watford, England, pp. 165-171.
- Mainstone RJ (1974). Supplementary Note on the Stiffness and Strengths of Infilled Frames. Building Research Station UK, Current Paper 13/74, February.
- Okuyucu D, Tankut (2009). Effect of Panel Concrete Strength on Seismic Performance of RC Frames Strengthened by Precast Concrete Panels. WCCE-ECCE-TCCE Joint Conference: earthquake & tsunami held at Istanbul, Turkey, IMO Publication Nr.: E/09/03, June 22-24.
- Paulay T, Priestley MJN (1992). *Seismic Design of Reinforced Concrete and Masonry Buildings*, New York, John Wiley.
- Polyakov SV (1957). *Masonry in Framed Buildings; An Investigation into the Strength and Stiffness of Masonry Infilling (English Translation)*, Moscow.
- Saneinejad A, Hobbs B (1995). Inelastic Design of Infilled Frames. *J. Struct. Eng.*, 121(4): 634-650.
- Seah CK (1998). *Universal Approach for the Analysis and Design of Masonry-Infilled Frame Structures*. Ph D Thesis, University of New Brunswick, Fredericton (NB), Canada.
- Sevil T (2010). *Seismic Strengthening of Masonry Infilled R/C Frames with Steel Fiber Reinforcement*. Ph D Thesis, Middle East Technical University, Ankara, Turkey.
- Sevil T, Baran M, Canbay E (2010). Investigation of the Effects of Hollow Brick Infills on the Behavior of Reinforced Concrete Framed Structures; Experimental and Analytical Studies. *International Journal of Research and Development*, Accepted for Publication.
- Sezen H, Moehle JP (2004). Shear Strength Model for Lightly Reinforced Concrete Columns. *J. Struct. Eng. ASCE*, 130: 1692-1703.
- Smith BS (1962). Lateral Stiffness of Infilled Frames. *ASCE J. Struct. Div.*, 88: 183-199.
- Smith BS (1966). Behaviour of Square Infilled Frames. *ASCE J. Struct. Div.*, 92, ST. 1.
- Smith BS (1967). Methods for Predicting the Lateral Stiffness and Strength of Multi-Storey Infilled Frames. *Build. Sci.*, 2: 247-257.
- Smith BS (1968). Model Test Results of Vertical and Horizontal Loading of Infilled Specimens. *ACI J.* August, pp. 618-624.
- Smith BS, Carter CA (1969). Method of Analysis for Infilled Frames. *Proc. ICE.*, pp. 44: 31-48.
- Turkish Seismic Code (2006). Ministry of Public Work and Settlement, Government of Republic of Turkey, Ankara.
- Uniform Building Code (1997). 5360 Workman Mill Road, Whittier, California 90601-2298, USA.